Cell Host & Microbe, Volume *28*

Supplemental Information

Real-Time Conformational Dynamics of SARS-CoV-2 Spikes on Virus Particles

Maolin Lu, Pradeep D. Uchil, Wenwei Li, Desheng Zheng, Daniel S. Terry, Jason Gorman, Wei Shi, Baoshan Zhang, Tongqing Zhou, Shilei Ding, Romain Gasser, Jérémie Prévost, Guillaume Beaudoin-Bussières, Sai Priya Anand, Annemarie Laumaea, Jonathan R. Grover, Lihong Liu, David D. Ho, John R. Mascola, Andrés Finzi, Peter D. Kwong, Scott C. Blanchard, and Walther Mothes

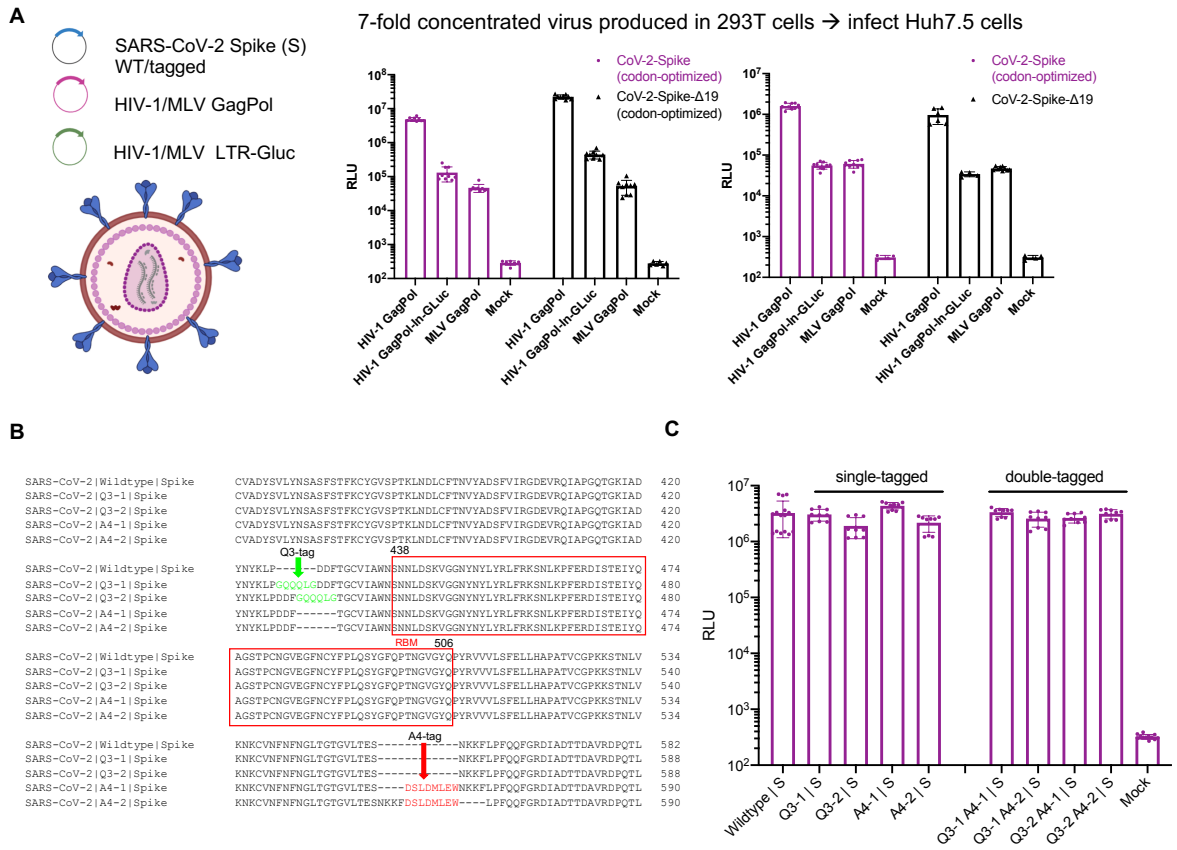

Figure S1. Single-tagged and double-tagged spike proteins for smFRET imaging retain infectivity. (Related to Figure 1).

(A) Establishment of infectivity assays using lentivirus (HIV-1) and retrovirus particles (MLV) carrying SARS-CoV-2 spike proteins. HIV-1 or MLV single-round viruses used for infectivity and neutralization assays were generated by transfecting HEK293T cells with plasmids expressing respective GagPol, LTR-intron Gaussia luciferase Gluc (Jin et al., 2009; Zhong et al., 2013) or plasmid encoding HIV-1 envelope-deleted genome encoding intron Gluc together with codon-optimized, or Δ19 (spike with 19 amino acids deleted from C-terminal) of SARS-CoV-2 spike (Johnson et al., 2020).

(B) Peptide insertion sites into RBD and SD1 before and after RBM to avoid interfering with receptor binding. Q3 tag was inserted at two positions (Q3-1 and Q3-2) on RBD, separately. A4 peptide tag was inserted at two sites (A4-1 and A4-2) on SD1.

(C) Infectivity of HIV-1 lentivirus carrying single-tagged and double-tagged spike proteins as determined on Huh 7.5 cells. Infectivity (mean ± s.d.) was measured from three independent experiments in triplicates. RLU, relative light units.

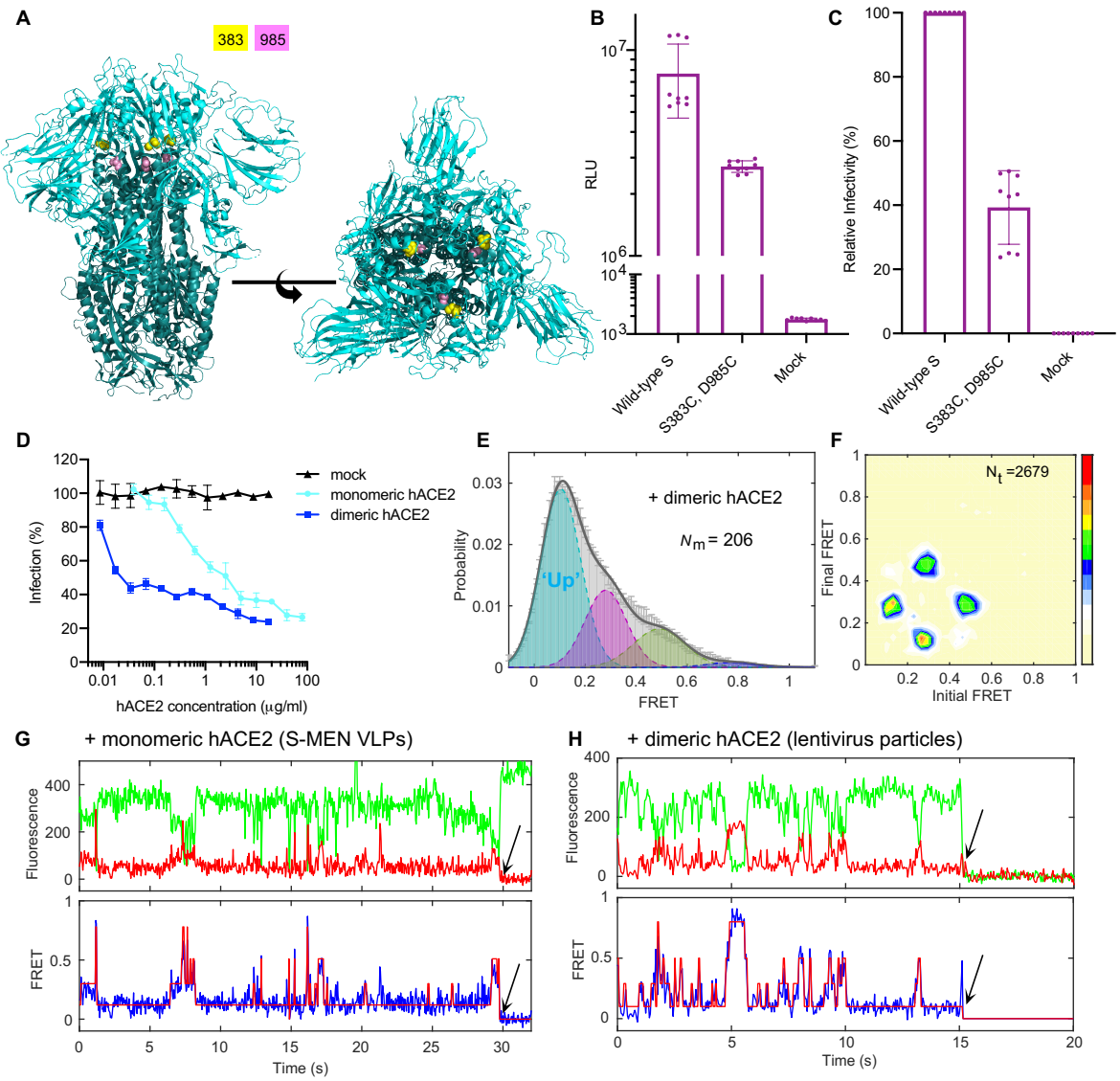

Figure S2. Stabilizing S by an introduced disulfide and activating S by dimeric hACE2. (Related to Figure 2).

(A–C) Relative infectivity of S containing S383C, D985C modifications.

(A) Structure (PDB: 6ZOY) of disulfide (S383C, D985C)-stabilized spike in all 'down' state (left panel: side view; right panel: top view; 383 site in yellow spheres; 985 site in pink spheres).

(B, C) Infectivity of spike mutant S383C, D985C in comparison to wildtype, represented as absolute RLU (B) and normalized (C) to wild-type (%). Infectivity (mean ± s.d.) was repeated three times in triplicates. RLU, relative light units.

(D–F) Dimeric hACE2 activates spike protein by stabilizing the low-FRET conformation.

(D) Dimeric hACE2 (containing the dimerization domain (residues 616-732) is more potent than monomeric hACE2. Infectivity of lentivirus particles carrying SARS-CoV-2 Spike in presence of indicated amounts of soluble monomeric or dimeric hACE2 protein using 293T cells stably expressing hACE2 as target cells. Experiment was performed in triplicates and represented as mean ± s.d.

(E, F) The FRET histogram (E) and the corresponding transition density plot (F) of spikes on lentivirus particles in the presence of 200 μg/ml dimeric hACE2. 206 (N_m) individual dynamic

traces were compiled into a conformation-population FRET histogram (gray lines, E) and fitted into a 4-state Gaussian distribution (solid black, E). Compared to monomeric hACE2, dimeric hACE2 further reduces the occupancy of the very high-FRET and facilitates the stabilization in the low-FRET receptor-stabilized state (F). FRET histograms represent mean ± s.e.m., determined from three randomly-assigned populations of all FRET traces. Evaluated state occupancies see Table S1.
(G, H) Additional example fluorescence traces (Cy3B, green; LD650, red) and resulting quantified low-FRET dominated traces (FRET efficiency, blue; hidden Markov model initialization, red) of spikes in the presence of monomeric (G) and dimeric hACE2 (H) on the surface of virus particles. Arrows point to the single-step photobleaching steps of dyes at the single-molecule level and define the baseline.

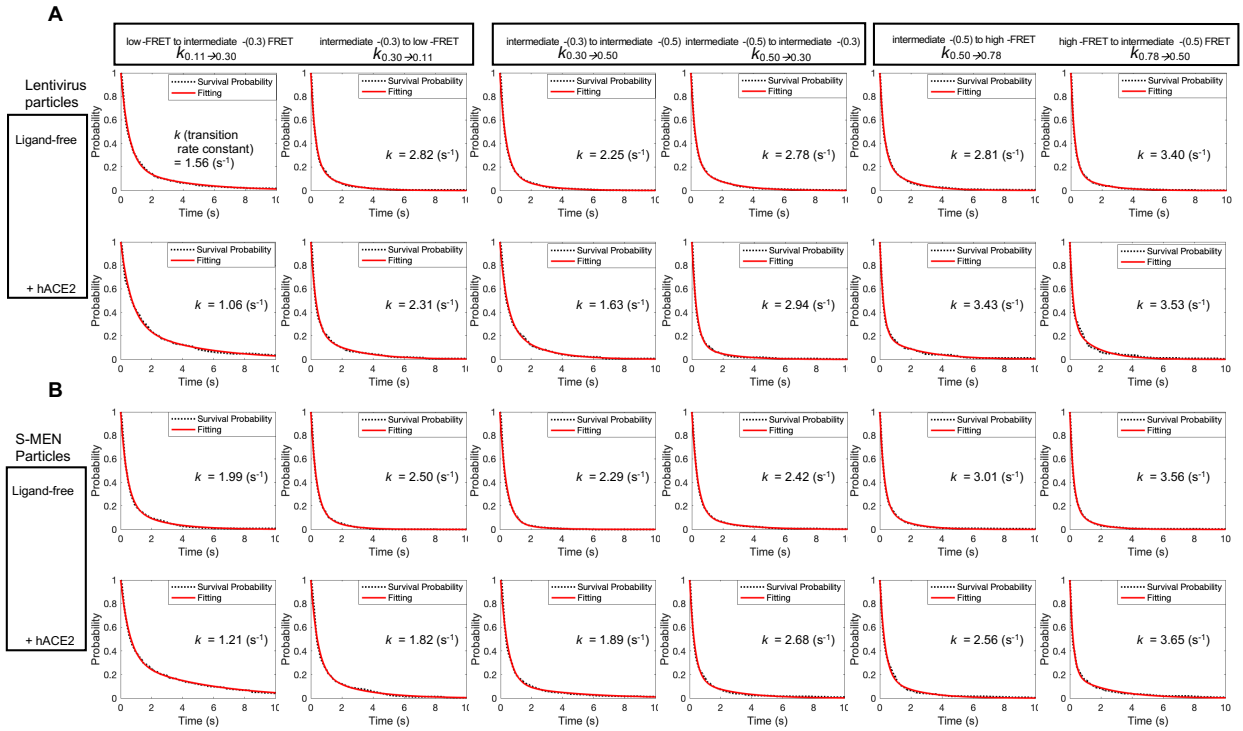

Figure S3. Kinetic analysis of spike proteins, and modulation by hACE2. (Related to Figure 2).

(A, B) Survival probability plots of conformational states of spikes on lentivirus particles (A) and on S-MEN (B) in the absence (ligand-free, top row) and the presence of 200 μg/ml hACE2 (bottom row). The survival probability plot is a function of time-duration of spikes dwelling on specific conformations before state-to-state transitions occur. Transition rates were derived from double exponential-fitting of survival probability plots and summarized in Table S2.

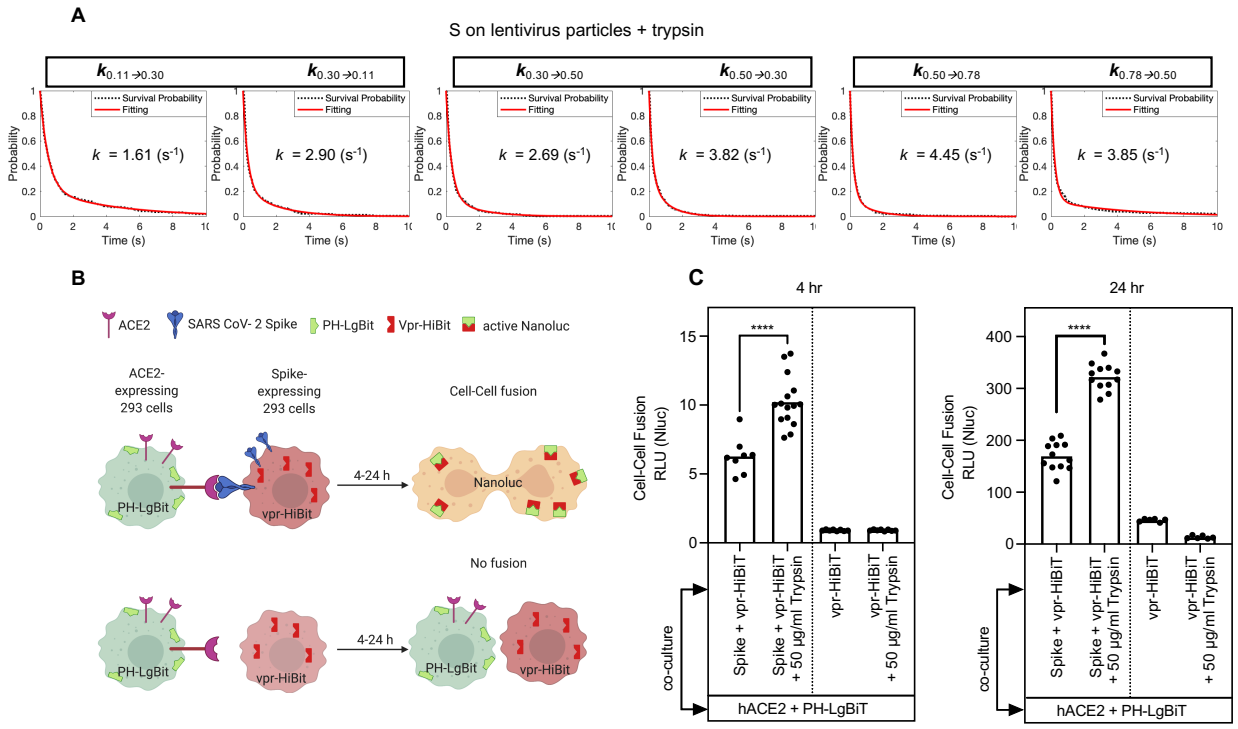

Figure S4. The effect of trypsin on conformational dynamics of SARS CoV-2 spike and on hACE2-SARS-CoV-2-mediated cell-cell fusion. (Related to Figure 3).

(A) Survival probability plots of spike-conformations in the presence of 50 µg/ml trypsin give rise to the calculation of transition rates among different conformations of spikes. Transition rates are summarized in Table S2.

(B, C) Effect of trypsin treatment on hACE2-SARS-CoV-2-mediated cell-cell fusion.

(B) Assay design to monitor cell-cell fusion using the HiBit and LgBiT split NanoLuc system (Yamamoto et al., 2019). HEK293 cells transiently expressing Vpr-HiBit with or without SARS-CoV-2 spike were co-cultured with HEK293 cells transiently expressing LgBiT tagged to PH domain of human phospholipase Cδ at the N-terminus together with hACE2. SARS-CoV-2 spike-hACE2-dependent cell-cell fusion was determined by monitoring reconstituted NanoLuc activity at 4 and 24 h post co-culture.

(C) Normalized relative luciferase units (RLU; bars denote mean; dots, individual data points of replicates) measured at 4 h and 24 h post co-culture to quantify cell-cell fusion in stated cell populations. Indicated cell populations were either left alone or treated with 50 µg/ml trypsin for 10 min at 37 °C before co-culture. Reconstituted NanoLuc activities were normalized to luciferase activity detected in cell populations without co-culture. p values were derived from unpaired t-test; **** denote $p < 0.0001$

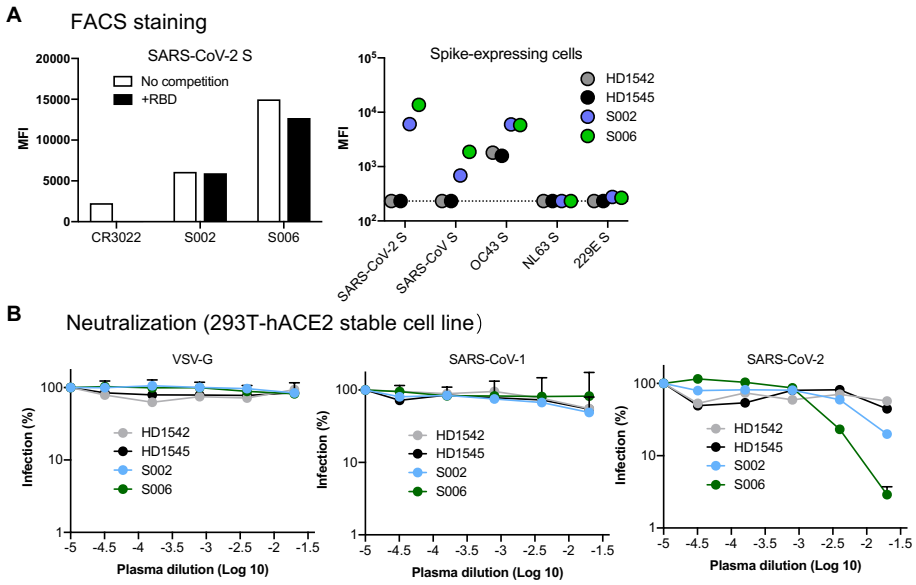

Figure S5. Convalescent plasma of SARS-CoV-2 positive patients S006 and S002 bind to S and neutralize SARS-CoV-2. (Related to Figure 4).

(A) FACS staining of SARS-CoV-2 S-expressing cells shows that both S006 and S002 bind to S.

(B) VSV-G (left), SARS-CoV-1 (middle), SARS-CoV-2 (right) lentivirus neutralization curves of plasma S006, S002, HD1542 and HD1545. Both S006 and S002 show virus neutralizing ability against lentiviruses carrying SARS-CoV-2 S. Neutralization curves represent mean ± s.d. from three replicates.

Table S1. Relative state-occupancy and fitting parameters in each of four FRET-defined conformational states of SARS-CoV-2 spike protein on the surface of virus particles. (Related to Figures 2, 3, 4, 5, and S2).

The FRET efficiency histograms were fitted into the sum of four Gaussian distributions (μ, the mean or expectation of the Gaussian distribution; σ, s.d. of the Gaussian distribution) for each conformational state. Parameters were based upon the observation of original FRET efficiency data and were further determined using hidden Markov modelling. Relative conformational state-occupancy of SARS-CoV-2 spike protein on viral particles are presented as mean ± s.e.m., determined from three independent measurements. R-squared values were evaluated to indicate the goodness of fit.

SARS-CoV-2 spikes on lentivirus particles	Curve fitting R-squared	**low-FRET**	**intermediate-(0.3) FRET**	**intermediate-(0.5) FRET**	**high-FRET**
		μ: 0.11+/-0.01	**μ**: 0.30+/-0.01	**μ**: 0.50+/-0.02	**μ**: 0.78+/-0.03
		σ: 0.08+/-0.01	**σ**: 0.08+/-0.01	**σ**: 0.10+/-0.01	**σ**: 0.10+/-0.01
Ligand-free	0.9921	22% +/- 7%	26% +/- 11%	38% +/- 12%	14% +/- 8%
+ hACE2	0.9966	48% +/- 10%	29% +/- 11%	17% +/- 12%	6% +/- 3%
+ dimeric hACE2	0.9968	58% +/- 8%	25% +/- 12%	16% +/- 11%	2% +/- 2%
+ trypsin	0.9808	28% +/- 9%	27% +/- 9%	28% +/- 9%	17% +/- 5%
+ trypsin + hACE2	0.9882	51% +/- 9%	24% +/- 11%	19% +/- 10%	5% +/- 8%
+ CR3022	0.9952	45% +/- 3%	24% +/- 10%	21% +/- 9%	10% +/- 7%
+ CR3022 + hACE2	0.9926	44% +/- 8%	28% +/- 13%	18% +/- 12%	10% +/- 8%
+ VHH72	0.9915	46% +/- 6%	25% +/- 12%	20% +/- 12%	9% +/- 4%
+ VHH72 + hACE2	0.9949	55% +/- 7%	20% +/- 9%	20% +/- 10%	5% +/- 7%
+ H4	0.9947	51% +/- 9%	22% +/- 12%	22% +/- 12%	5% +/- 6%
+ H4 + hACE2	0.9966	53% +/- 8%	20% +/- 12%	21% +/- 13%	6% +/- 4%
+ S002	0.9958	23% +/- 5%	20% +/- 12%	45% +/- 12%	12% +/- 6%
+ S002 + hACE2	0.9904	41% +/- 7%	24% +/- 12%	24% +/- 12%	11% +/- 4%
+ S006	0.9930	54% +/- 11%	24% +/- 12%	16% +/- 10%	6% +/- 3%
+ S006 + hACE2	0.9955	51% +/- 10%	25% +/- 12%	19% +/- 13%	5% +/- 5%
+ 2-4	0.9907	25% +/- 10%	20% +/- 13%	45% +/- 11%	10% +/- 5%
+ 2-4 + hACE2	0.9959	39% +/- 10%	29% +/- 13%	26% +/- 12%	6% +/- 5%
+ 2-43	0.9925	35% +/- 3%	28% +/- 11%	25% +/- 8%	12% +/- 5%
+ 2-43 + hACE2	0.9906	52% +/- 9%	22% +/- 13%	22% +/- 13%	4% +/- 5%
S383C, D985C ligand-free	0.9933	20% +/- 5%	18% +/- 11%	45% +/- 12%	17% +/- 7%

SARS-CoV-2 spikes on S-MEN	Curve fitting R-squared	**low-FRET**	**intermediate-(0.3) FRET**	**intermediate-(0.5) FRET**	**high-FRET**
		μ: 0.11+/-0.01	**μ**: 0.30+/-0.01	**μ**: 0.50+/-0.02	**μ**: 0.78+/-0.03
		σ: 0.08+/-0.01	**σ**: 0.08+/-0.01	**σ**: 0.10+/-0.01	**σ**: 0.10+/-0.01
Ligand-free	0.9886	26% +/- 6%	23% +/- 11%	39% +/- 12%	12% +/- 7%
+ hACE2	0.9977	49% +/- 8%	24% +/- 11%	20% +/- 11%	7% +/- 6%

Table S2. Transition rates between observed conformational states of SARS-CoV-2 spike on virus particles. (Related to Figures 2, 3, S3, and S4).

The survival probability plots (Figures S3 and S4) were derived from distributions of dwell times for each state-to-state transition determined through Hidden Markov Modeling (HMM). Then plots were fitted by double-exponential distributions: $y(t) = A_1 \exp^{-k1t} + A_2 \exp^{-k2t}$), where $y(t)$ is the probability and t is the dwell time. The presented rates were the weighted average of two rates derived from double-exponential decays. Rates were finally presented in the table as (*weighted average +/- 95% confidence intervals*).

SAR-CoV-2 Spikes on virus particles	$k_{0.11\rightarrow0.30}$ (s^{-1})	$k_{0.30\rightarrow0.11}$ (s^{-1})	$k_{0.30\rightarrow0.50}$ (s^{-1})	$k_{0.50\rightarrow0.30}$ (s^{-1})	$k_{0.50\rightarrow0.78}$ (s^{-1})	$k_{0.78\rightarrow0.50}$ (s^{-1})
Retroviral pseudo-particles						
Ligand-free	1.56 +/- 0.01	2.82 +/- 0.03	2.25 +/- 0.03	2.78 +/- 0.02	2.81 +/- 0.02	3.40 +/- 0.03
+ hACE2	1.06 +/- 0.01	2.31 +/- 0.03	1.63 +/- 0.03	2.94 +/- 0.03	3.43 +/- 0.04	3.53 +/- 0.07
S-MEN particles						
Ligand-free	1.99 +/- 0.02	2.50 +/- 0.04	2.29 +/- 0.04	2.42 +/- 0.01	3.01 +/- 0.03	3.56 +/- 0.03
+ hACE2	1.21 +/- 0.01	1.82 +/- 0.02	1.89 +/- 0.02	2.68 +/- 0.03	2.56 +/- 0.03	3.65 +/- 0.04